THE JOURNAL OF PHYSICAL CHEMISTRY B

Article

pubs.acs.org/JPCB

Mechanical Behavior of a *Bacillus subtilis* Pellicle

Emily C. Hollenbeck,[†] Carine Douarche,[‡] Jean-Marc Allain,[§] Philippe Roger,[∥] Christophe Regeard,[⊥] Lynette Cegelski,[#] Gerald G. Fuller,[†] and Eric Raspaud*[,‡]

[†]Department of Chemical Engineering, Stanford University, Stanford, California 94305, United States

[‡]Laboratoire de Physique des Solides, CNRS, Université Paris-Sud, Université Paris-Saclay, Orsay, France

[§]Laboratoire de Mécanique des Solides, École Polytechnique, CNRS, Université Paris-Saclay, Palaiseau, France

[∥]Institut de Chimie Moléculaire et des Matériaux d'Orsay (ICMMO), CNRS, Université Paris-Sud, Université Paris-Saclay, Orsay, France

[⊥]Institut de Biologie Intégrative de la Cellule (I2BC), CEA, CNRS, Université Paris-Sud, Université Paris-Saclay, Gif sur Yvette, France

[#]Department of Chemistry, Stanford University, Stanford, California 94305, United States

ABSTRACT: Bacterial biofilms consist of a complex network of biopolymers embedded with microorganisms, and together these components form a physically robust structure that enables bacteria to grow in a protected environment. This structure can help unwanted biofilms persist in situations ranging from chronic infection to the biofouling of industrial equipment, but under certain circumstances it can allow the biofilm to disperse and colonize new niches. Mechanical properties are therefore a key aspect of biofilm life. In light of the recently discovered growth-induced compressive stress present within a biofilm, we studied the mechanical behavior of *Bacillus subtilis* pellicles, or biofilms at the air−liquid interface, and tracked simultaneously the force response and macroscopic structural changes during elongational deformations. We observed that pellicles behaved viscoelastically in response to small deformations, such that the growth-induced compressive stress was still present, and viscoplastically at large deformations, when the pellicles were under tension. In addition, by using particle imaging velocimetry we found that the pellicle deformations were nonaffine, indicating heterogeneous mechanical properties with the pellicle being more pliable near attachment surfaces. Overall, our results indicate that we must consider not only the viscoelastic but also the viscoplastic and mechanically heterogeneous nature of these structures to understand biofilm dispersal and removal.

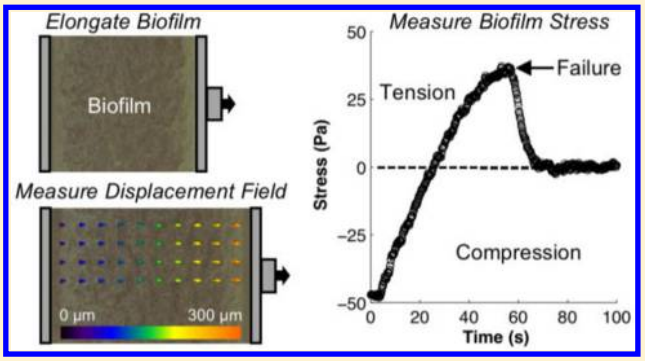

INTRODUCTION

Bacterial biofilms—communities of bacteria embedded in an extracellular matrix of biopolymers—are living systems with a heterogeneous, multicomponent structure. This makes the mechanical characterization of such systems a challenge as compared to inert, chemically defined materials. However, understanding biofilm mechanics is highly important because it is often structural robustness that allows biofilms to persist[1] or structural failure that allows biofilms to disperse and colonize new niches,[2] a part of the biofilm lifecycle essential to bacterial survival. While mechanical properties are therefore a key aspect in allowing biofilms to be an integral part of the natural environment, in some cases they contribute to detrimental aspects of the biofilm lifestyle. For example, biofilm dispersal can lead to disease transmission, such as the transmission of an environmental pathogen to the human host, or spread of infection within the host.[2] In addition, the robustness of the biofilm structure promotes bacterial colonization of indwelling medical devices and the development of chronic infections,[3−5] biofilm growth on food processing equipment and in drinking water systems,[6] and biofouling of pipelines, ship hulls, and other industrial equipment.[7] Conversely, if we can understand and control the mechanical properties, this offers a strategy to combat unwanted biofilms. This is an attractive option considering that microorganisms embedded in biofilms are often highly resistant to biocides and are therefore difficult to clear by chemical means alone.[8] For example, novel therapeutics that promote biofilm detachment such as matrix-degrading enzymes that weaken the biofilm structure are under investigation to treat biofilm-related infections.[9,10] Overall, increasing our general knowledge of biofilm mechanics will help us to better understand the fundamentals of biofilm persistence and dispersal while supporting the development of controlled removal strategies.

Special Issue: William M. Gelbart Festschrift

Received: February 28, 2016
Revised: April 5, 2016

DOI: 10.1021/acs.jpcb.6b02074
J. Phys. Chem. B XXXX, XXX, XXX−XXX

The extracellular portion of a biofilm is a hydrated matrix composed of polysaccharides and proteins, lipids, and nucleic acids that are secreted by the bacteria and arranged in an intricate structure. Specifically, *Bacillus subtilis*, a commonly studied model organism for biofilm formation, secretes an extracellular matrix containing polysaccharides, amyloid fibers, and hydrophobic proteins[11−14] and is capable of forming biofilms at the air−liquid interface, termed pellicles. Characterizing biofilms as soft complex materials is now widely appreciated,[15] and numerous studies have shown that biofilms are viscoelastic materials that display both viscous and elastic responses to mechanical deformation.[16] These studies have primarily focused on measuring mechanical properties by subjecting biofilms to small forces and deformations such that the material structure is not significantly altered.[17−19] On the other hand, few investigations have been performed that measure the mechanical properties of biofilms subjected to large deformations or that explore irreversible—or plastic—changes to the biofilm structure. While the research to date has provided tremendous understanding of biofilm material properties, if we want to gain insight into the mechanics of biofilm dispersal and removal, we must also consider the effects of large forces and deformations that approach biofilm rupture and/or detachment from surfaces.

One unique property of biofilms compared with traditional materials is the ability to create growth-induced compressive stress, which has been both theorized[19] and recently demonstrated experimentally.[20] Compression in biological systems can offer advantageous properties. For example, packaging of DNA in some bacteriophage capsids creates an internal pressure that aids in DNA ejection. Since ejection of bacteriophage DNA can be prevented when the external environment has a sufficient osmotic pressure,[21−23] high pressurization inside the capsid creates a driving force that can overcome this resisting force. Analogously, biofilms can generate an internal compressive stress arising from growth in a confined space. This compressive stress allows the biofilm to expand in area once the external constraints are released, which provides potential advantages such as facilitating self-repair if the film is ruptured.[20] However, we currently have little understanding of the effect of this internal compressive stress on the mechanical properties of the biofilm.

In this work, we focus on two largely unexamined areas of biofilm mechanics: the properties of biofilms subjected to large deformations and the effect of the recently discovered growth-induced compressive stress on the biofilm mechanical response. To do this, we used a custom-built apparatus to characterize the mechanical properties of *B. subtilis* pellicles subjected to elongational deformations (Figure 1). Pellicles were grown at the air−medium interface for 2 days and allowed to naturally attach to two plates partially submerged in the medium, one that is attached to a translation stage and used to stretch the pellicle and another that is attached to a force sensor. Natural attachment to the plates allowed for minimal perturbation to the pellicle structure prior to the measurement. Additionally, we imaged from the top during elongation and used this to determine the local deformation field of the pellicle. Overall, pellicles exhibited viscoelastic behavior at small deformations, when the internal compressive stress was still present, and viscoplastic behavior at large deformations, once the compressive stress was relieved and pellicles were under tension. Particle image velocimetry (PIV) analysis of macroscale pellicle images additionally revealed that the deformation

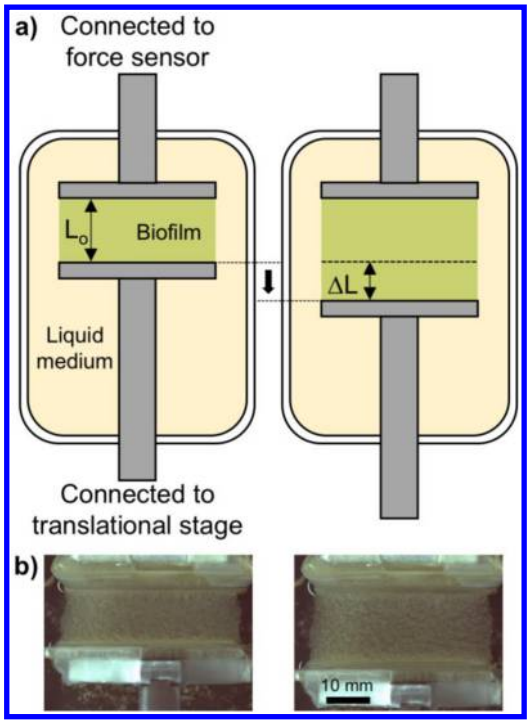

Figure 1. (a) Top-view schematic diagram and (b) images of the experimental setup used to elongate *B. subtilis* pellicles and record the mechanical response. The pellicle initially covered the entire air−liquid interface. Right before the experiment, excess pellicle was trimmed away to elongate only the material remaining between the two plates. One plate was connected to a force sensor and the other to a translational stage.

field of the pellicle was nonuniform, which suggests that the mechanical properties of the pellicle are also nonuniform. We observed that the pellicle is more pliable near attachment surfaces and calculated local properties of the biofilm using our PIV results. Whereas previous studies have focused on the viscoelastic and average properties of biofilms, our results show that if we want to understand large deformations and biofilm dispersal or removal, we must also appreciate the viscoplastic and nonuniform nature of these naturally grown structures.

MATERIALS AND METHODS

Bacterial Culture. A single colony of *B. subtilis* wild-type strain NCIB3610 was isolated from an agar plate and grown overnight in LB medium (10 g of NaCl, 5 g of yeast extract, and 10 g of tryptone per liter) at 30 °C under 240 rpm shaking. Fresh colonies were prepared every 2 weeks by streaking agar plates with a −80 °C bacterial stock. The overnight culture was diluted 1:1000 into 5 mL of LB and incubated under the same conditions until reaching an optical density at 600 nm (OD_{600}) of 0.1. This culture was then used to inoculate 25 mL of a biofilm medium (LB supplemented with 0.1 mM $MnCl_2$ and 3% glycerol) in a 6.1 cm × 4.6 cm rectangular dish to an OD_{600} of 10^{-3}. The culture was placed in a biosafety cabinet at 23 °C, and the sterilized plates of the experimental setup were submerged vertically into the medium 1−2 mm so that the pellicle could naturally attach to the plates during growth. After approximately 48 h a relatively smooth pellicle with no large folds formed, at which point the experiments were conducted. Right before the experiment, excess pellicle was trimmed away so that material remained only between the two plates and at the air−liquid interface. In most cases experiments were

DOI: 10.1021/acs.jpcb.6b02074
J. Phys. Chem. B XXXX, XXX, XXX−XXX

performed in triplicate, and a representative trial illustrating the phenomena common to all trials is given in each figure. Overall, more than 100 biofilms were studied over the past 5 years.

Experimental Apparatus. The lab-built apparatus used for the mechanical measurements in this study has been described previously.[19,20] Briefly, as the pellicle grew, it naturally attached to two plastic plates made of poly(ethylene terephthalate). One plate was attached to a mobile stage (Physik Instrumente GmbH & Co. KG, Karlsruhe, Germany) that could be moved back and forth to stretch the pellicle. The other plate was attached to a precalibrated double-cantilever spring (spring constant ~20 N/m) placed in front of a capacitive gauge (Fogale Nanotech, Nîmes, France). As the pellicle was stretched, it generated a force on the plate attached to the double-cantilever spring and displaced it slightly, on the order of microns. This displacement was calculated from the capacitive gauge voltage, and therefore, the force on the plate could be calculated using the spring constant. The standard error of the force data was less than 5%. A negative force value meant the pellicle was pushing on the plate. Stress values were calculated by dividing the force by the contact area between the pellicle and the plate, equal to the width of the plate multiplied by the thickness of the pellicle (350 ± 50 μm).[20] The applied strain was calculated as the change in the length of the pellicle divided by its original length (i.e., $\Delta L/L_o$, as defined in Figure 1). In most of the experiments, the original length L_o was on the order of 12 mm.

Image Analysis. A digital camera (Sony) was mounted over the setup, and top-view videos were recorded as the pellicles were stretched. Videos were analyzed using the PIV plugin of ImageJ to obtain the displacement field of the stretched pellicle. While the PIV method is typically applied to fluids containing tracer particles, we found that the grainy texture of the pellicle provided sufficient contrast. PIV analysis calculates the displacement field between two images, and therefore, each pair of video frames was analyzed, i.e., the displacement field from frame 1 to frame 2, the displacement field from frame 2 to frame 3, etc. The method divides each video frame into small interrogation sections and finds the average displacement per section when comparing two consecutive video frames. The average displacement for each interrogation section is indicated by a vector. After obtaining displacement fields for the entire video, we could then determine the total strain for a specific spatial section of the pellicle.

RESULTS AND DISCUSSION

Monitoring Pellicle Stress through Structural Failure Confirms the Presence of Growth-Induced Compressive Stress. As an aim of this study was to understand biofilm mechanics for situations relevant to biofilm dispersal and removal, we used our apparatus to deform *B. subtilis* pellicles to the point of structural failure. A representative stress curve for a pellicle that underwent failure is given in Figure 2b, with the applied strain shown above in Figure 2a. In this case, the pellicle started to detach from the plates of the apparatus at around 60 s and a strain of 0.4 and fully detached within the next 10 s. This detachment allowed us to define the point of zero stress, as there were no longer any horizontal forces acting on the plates. This was necessary because we could measure only relative changes in the stress—the initial value measured at the start of the experiment was arbitrary. By applying this zero-stress definition, we found that at the start of the experiment

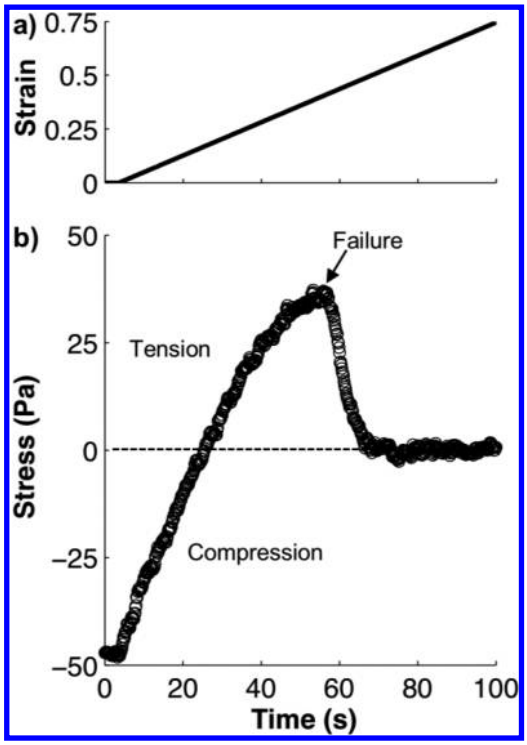

Figure 2. Elongation of a *B. subtilis* pellicle past structural failure. The pellicle was elongated at a constant rate of applied strain (a) while the force was measured. Stress values were then calculated from the measured force (b). A stress drop followed pellicle failure (observed after 60 s in the present case). The point at which the pellicle was no longer attached to the apparatus plates was used to define zero stress.

the pellicle was already under compression, approximately −50 Pa. This confirmed the results of our previous study that demonstrated the presence of internal compressive stress in a pellicle[20] and allowed us to appropriately shift our data to the correct absolute stress values. It should be noted that in our previous study, the average internal compressive stress was −80 Pa with a high deviation of ±25 Pa.[20] In performing multiple trials during this study, we also observed that the internal compressive stress varied from pellicle to pellicle and exhibited large variations (from −20 to −90 Pa). The curve in Figure 2b is therefore representative of the trend observed in all of the trials with an initial value that may change from one sample to another. The stress curves obtained from these experiments also revealed that we need to apply relatively large strains of ~0.1−0.2 for the pellicle to be under tension. For all of the experiments presented in this paper, pellicles were stretched past failure at the end of the experiment to determine the point of zero stress, although for clarity the failure event may not be shown in each plot.

Deformations in the Compressive Regime Are Reversible But Become Irreversible When the Pellicle Is under Tension. To understand the mechanical behavior of the *B. subtilis* pellicle at small versus large deformations, we elongated and compressed the pellicle in a cyclic manner to increasingly larger strain values. Figure 3a shows the results of an experiment in which a pellicle, starting at a growth-induced compressive stress of approximately −57 Pa, underwent five cycles of elongation and compression first to 0.05 strain (blue curves), then 0.1 strain (red curves), then 0.2 strain (green curves), and finally 0.3 strain (purple curves) in one continuous experiment for a total of 20 cycles. For the low-strain cycles

DOI: 10.1021/acs.jpcb.6b02074
J. Phys. Chem. B XXXX, XXX, XXX−XXX

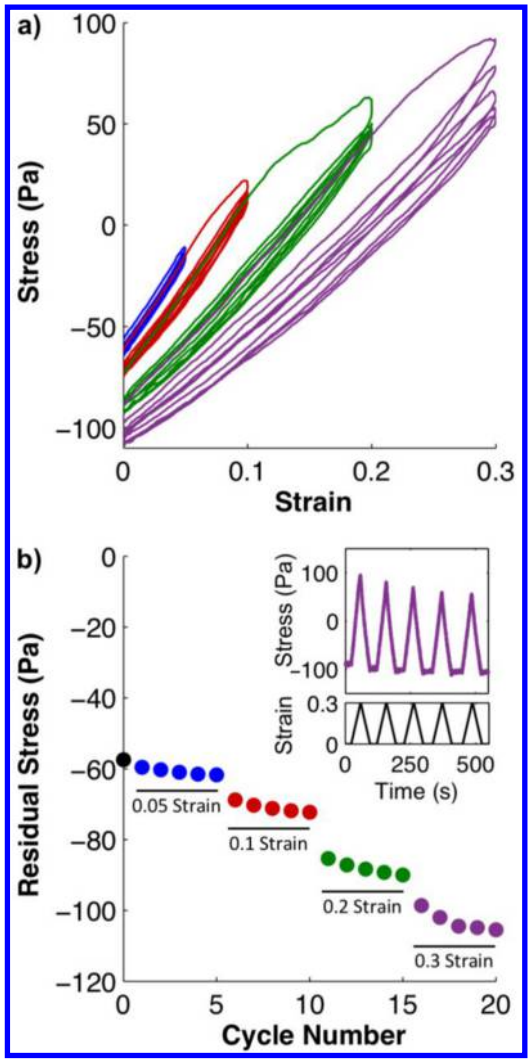

Figure 3. (a) Cyclic loading of a *B. subtilis* pellicle: 0.05 strain (blue curves), 0.1 strain (red curves), 0.2 strain (green curves), and 0.3 strain (purple curves). (b) The growth-induced compressive stress was measured before loading (black circle), and the residual stress was measured after each cycle (colored circles). The inset shows the measured stress and applied strain over time for five of these cycles (0.3 strain).

(out to 0.05), the elongation and compression curves closely coincided and no significant hysteresis was observed, indicating that this process is reversible and the pellicle structure is not significantly altered by a strain of 0.05. However, when the pellicle was elongated to strain values of 0.1 and higher, it exhibited different mechanical behavior. These higher-strain cycles displayed hysteresis, with the largest hysteresis occurring for the first cycle at each level of strain. Additionally, the elongation and compression curves of subsequent cycles did not coincide, but instead, the elongation curve of one cycle closely followed the compression curve of the previous cycle. In other words, each time the pellicle was stretched it reached lower stress values for the same applied strain compared with the previous cycle; such behavior is often called cyclic softening. This effect diminished with continued cycling at the same strain, as did the hysteresis. However, once the strain was increased to a new level, we again observed large hysteresis for the first cycle at that level. Overall, the different mechanical response of successive cycles indicates that the structure of the pellicle is altered—within the time scale of the experiment—by these larger deformations. Furthermore, the majority of the structural change happens the first time the pellicle is stretched to a certain strain level, as indicated by the observation that the largest hysteresis occurred during these cycles.

In addition to the observed hysteresis, another characteristic of this experiment was the pellicle stress measured after each cycle, termed the residual stress in Figure 3b. The inset in Figure 3b shows data from five elongation and compression cycles as a function of time for a strain of 0.3. We observed that after each cycle, when the pellicle was at a strain of zero, the stress returned to a value lower than that in the previous cycle. These values are plotted in Figure 3b for all of the cycles presented in Figure 3a. While the cycles to a strain of 0.05 caused a slight decrease of 4−7% in the residual stress compared with the initial growth-induced stress of approximately −57 Pa (black circle at cycle zero), at larger strains we observed a much lower residual stress than the original growth-induced stress and a decrease in the residual stress for cycles repeated at the same strain. For example, the residual stress was 19% lower than the initial growth-induced compressive stress after the first cycle at 0.1 strain and 26% lower after the final cycle at 0.1 strain. Additionally, increasing from 0.05 to 0.1 strain, 0.1 to 0.2 strain, and 0.2 to 0.3 strain caused a large decrease in the residual stress of approximately 10 Pa. These observations further support the idea that at 0.05 strain the pellicle structure is not significantly altered, as approximately the original growth-induced stress is reached upon completion of each elongation−compression cycle. However, at higher strains the structure must be altered with each cycle because of the decreasing residual stress values, with the most structural change occurring when the level of strain is increased. Additionally, we hypothesize that the residual stress decreased with successive cycles because of an elongation of the pellicle structure at high strains, such that when the pellicle was compressed to its initial starting length it pushed harder against the force sensor. These results demonstrate that in addition to growth in a confined space, applied mechanical stress is another mechanism by which internal stress may be generated within the pellicle. Interestingly, mechanically induced residual stress is on the order of growth-induced residual stress only after multiple deformation cycles at a high strain.

It should be noted that the data described above exhibit the Mullins effect,[24] a specific mechanical response first observed in rubbers displaying hysteresis and cyclic softening. Specifically, this effect is characterized by diminished hysteresis and cyclic softening for repeated cycles at the same strain and renewed hysteresis once a higher level of strain is applied. In recent years several groups have observed this effect in biological tissues, including caterpillar muscle,[25,26] mouse skin,[27] guinea pig small intestine,[28] and human aorta.[29] To our knowledge, this is the first observation of this phenomena in bacterial biofilms. Although several theories have been proposed to explain the Mullins effect, including both reversible or viscoelastic effects and irreversible structural damage, a molecular-level understanding remains elusive.[30]

Because of the known viscoelastic nature of biofilms, we sought to understand whether the altered mechanical response and potential structural change of the pellicle after large deformations was viscoelastic in nature, and therefore potentially reversible with time, or plastic and irreversible. Interestingly, we also noted that for cycles performed with the pellicle always under compression (positive stress values were

DOI: 10.1021/acs.jpcb.6b02074
J. Phys. Chem. B XXXX, XXX, XXX−XXX

not reached), the elongation−compression curves were coincident and unvarying, but once the pellicle was in tension (positive stress values were reached) we started to observe hysteresis, cyclic softening, and decreasing residual stress. As a result of these observations, we performed relaxation experiments to probe the viscoelastic versus plastic nature of pellicles that were deformed within these two regimes. The experiment in Figure 4a was performed on a pellicle that, unlike other

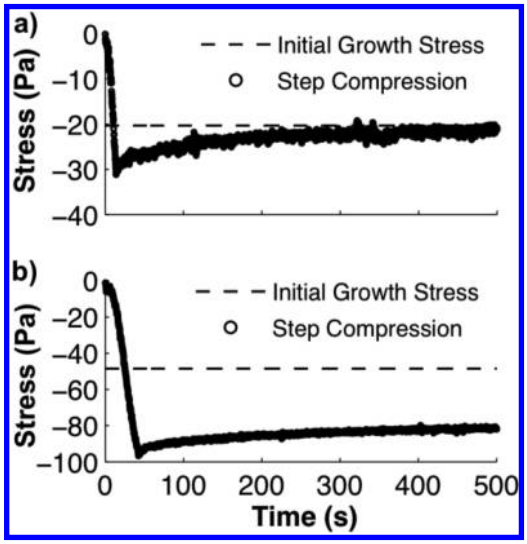

Figure 4. After experiencing different mechanical forces, pellicles were recompressed, and the stress relaxation was monitored over time. Specifically, pellicles were either (a) allowed to reach a state of zero internal stress without an applied mechanical force or (b) stretched to a state of tension by an applied mechanical force and then detached prior to recompression. The dashed line indicates the initial growth-induced compressive stress of the pellicle before the experiment was performed.

experiments, was manually cut from both plates prior to the experiment. It should be noted that severing the attachment between the pellicle and the plates did not change the initial growth-induced compressive stress within the pellicle. When the mobile plate was then retracted, the growth-induced compressive stress was relieved and the pellicle expanded, but the pellicle was not stretched beyond a state of zero stress, defined as the point when the pellicle no longer contacted the plates (this portion of the experiment is not shown in the figure). We then recompressed the pellicle to its original length and monitored the stress over time; the data corresponding to this portion of the experiment are shown in Figure 4a. We observed that when the pellicle reached its original length, the pellicle stress was at a minimum of −30 Pa, which was lower than the initial growth-induced compressive stress (dotted line). However, in a time-dependent manner, the pellicle could relax back to its initial growth-induced compressive stress, implying that this "decompression" process is reversible. In repeated experiments, this relaxation time was typically on the order of a few hundred seconds. Furthermore, the pellicle did not relax past its initial growth-induced stress toward a state of zero stress, indicating a return to the structure formed under the compressed state. On the other hand, for the experiment in Figure 4b, we first kept the pellicle attached to the plates so that it was stretched to a state of tension (∼+80 Pa), at which point it was then detached and no longer contacted the plates, defining the point of zero stress (this portion of the experiment is not shown in the figure). Upon recompression to its original length, we observed that the stress in the pellicle again reached a minimum (−100 Pa) but did not relax back to the original growth-induced compressive stress (dotted line) over time. This indicates that the pellicle structure changes in an irreversible manner under these higher tensions, and therefore, plastic deformations are likely significant in this regime. Overall, we conclude that if a pellicle remains under compression, deformations are reversible with time, primarily as a result of viscoelastic contributions, but once the pellicle is under tension, deformations can include a plastic component. Interestingly, this also implies that the yield point of the pellicle corresponds to a state near zero stress. In addition, it should be noted that these deformations are not perfectly plastic, as the stress does not become independent of the strain after yielding (Figure 3a) but instead exhibits strain-hardening behavior.

Pellicles Are Viscoelastic under Compression and Viscoplastic under Applied Tension. To further probe the time dependence of the pellicle mechanical response, we performed elongational deformations at different rates of strain. Figure 5a shows the stress−strain curves for separate pellicles stretched at rates of 1.6×10^{-4} to 7.3×10^{-2} s^{-1}, a range covering almost 3 orders of magnitude. We observed that the pellicle stress depended on the strain rate and that higher strain rates correlated to higher stress values for the same applied strain, which is consistent with the pellicle being a viscoelastic material.[31] Additionally, this trend is consistent with previous studies on biofilm mechanics.[32,33]

As demonstrated in the inset of Figure 5a, we calculated the tangent modulus by fitting the data to a straight line and determining the slope at both low strains (0−0.05), when the pellicles were under compression, and high strains (0.2−0.3), when the pellicles were under tension. These moduli are plotted in Figure 5b. Although an increase in the modulus was clearly observed with increasing rate of strain, for both low and high strains this dependence was weak. For example, while the strain rate increased almost 3 orders of magnitude, the moduli increased by less than a factor of 2. As summarized by Fung,[34] a variety of soft biological tissues display a similar trend for strain rates spanning several orders of magnitude; these tissues are considered relatively insensitive to strain rate. The dependence of the pellicle properties on the strain rate implies that there is a time-dependent viscous component to the mechanical behavior at both low and high strains; however, the fact that this dependence is weak indicates that the viscous contribution is small. A viscous component at low strains is consistent with our conclusion that the pellicle is viscoelastic while in a compressed state. Furthermore, as we have shown that pellicles can deform plastically under tension, the viscous contribution at high strains indicates that pellicles under tension may be better described as viscoplastic.

The viscous contributions at both low and high strains were further examined by means of stress relaxation experiments. As shown in Figure 6, we elongated pellicles to different amounts of strain, such that the pellicle was still under compression (0.05 strain) or reached a state of tension (0.25 strain), and tracked the stress evolution. In both strain regimes, the pellicle exhibited stress relaxation, regardless of whether it was in a state of compression or tension, further confirming that the pellicle behaves viscoelastically at low strains and viscoplastically at high strains. Furthermore, when the pellicle was stretched to a state of tension, it relaxed back to a negative stress value, meaning that it returned to a state of compression. These

DOI: 10.1021/acs.jpcb.6b02074
J. Phys. Chem. B XXXX, XXX, XXX−XXX

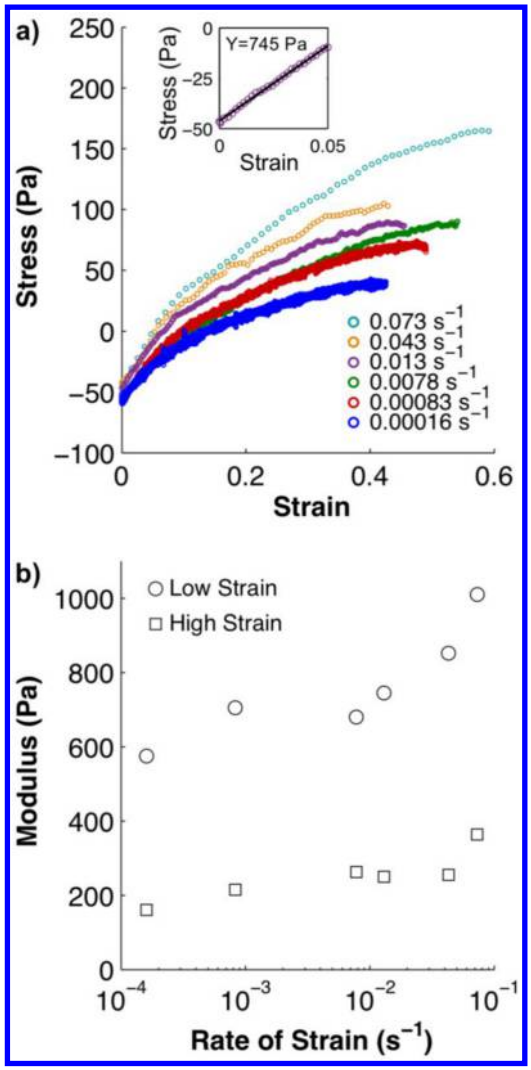

Figure 5. (a) Stress−strain curves for pellicles elongated at different rates of strain and (b) the tangent modulus calculated from these curves for both low strain (0−0.05) and high strain (0.2−0.3). The inset in (a) gives an example of a linear fit used to obtain the tangent modulus.

observations indicate that when deformed, the pellicle relaxes back toward a compressed state. This is likely due to the innate arrangement of the pellicle structure as it formed under compression during growth. It should be noted that we were not able to observe a complete return to the initial growth-induced compressive stress because at long times the growth of the pellicle interfered with the relaxation measurement (data not shown). However, these measurements did reveal that at short time scales the pellicle returns to a compressed state after deformation by a mechanism that is independent of growth.

In addition, we observed that the stress relaxation profiles did not fit a single-exponential decay but were better fit by a sum of exponentials. This is consistent with results from other studies specifically designed to probe biofilm stress relaxation.[35,36] This type of relaxation was also reported by Fung for a variety of biological tissues.[34] As suggested in these studies, this shows that multiple relaxation processes occur on different time scales to relieve the mechanically induced stress and in this case return to a compressed state.

The Pellicle Is Structurally Heterogeneous and More Pliable near Attachment Surfaces. In contrast to previous

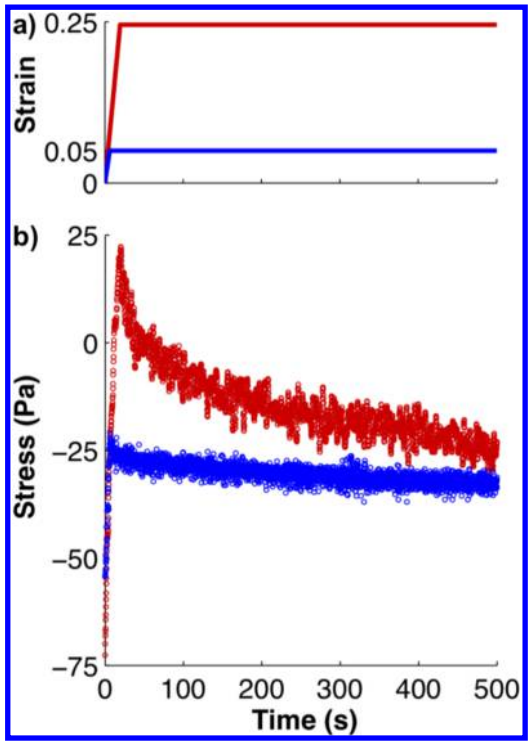

Figure 6. Pellicles were elongated to different amounts of applied strain (a), and the stress relaxation was monitored over time (b). In one case the pellicle initially reached a state of tension (0.25 strain, red curve) and in the other case always remained in a state of compression (0.05 strain, blue curve).

studies that applied small deformations so as to not significantly affect the biofilm structure, our experiments involved large deformations that altered the pellicle, in some cases irreversibly. We therefore sought to determine how the pellicle structure deformed while being stretched and whether this occurred in a homogeneous manner. To investigate this, we mounted a camera above the custom-built apparatus and recorded top-view videos of the pellicles as they were elongated during each experiment. We then determined the deformation field of the pellicle using PIV (see Materials and Methods).

The left panel of Figure 7 shows an experiment in which a pellicle was stretched between a stationary left plate and a mobile right plate. A vector field representing the PIV results for two consecutive video frames was superimposed on the pellicle image. As was anticipated, the vector field pointed in the direction of the pellicle elongation, but by plotting the displacement magnitude versus the position along the pellicle (Figure 7, center panel), we observed that the displacement profile was nonlinear. This means that the pellicle deformation is nonaffine, as an affine deformation would yield a displacement profile that is linear in position along the pellicle (dashed line). Because the local slope of the displacement profile gives the local strain experienced by the pellicle, these data indicate that the regions of the pellicle near the plates experience a larger strain than the center region.

As the applied force throughout the pellicle was uniform but the strain was not, this suggests that the mechanical properties of the pellicle are heterogeneous. Specifically, the edges of the pellicle near the attachment surfaces are more pliable, as these regions stretch more under the same applied force. Furthermore, heterogeneous mechanical properties indicate that there must be some nonuniformity in the pellicle structure.

DOI: 10.1021/acs.jpcb.6b02074
J. Phys. Chem. B XXXX, XXX, XXX−XXX

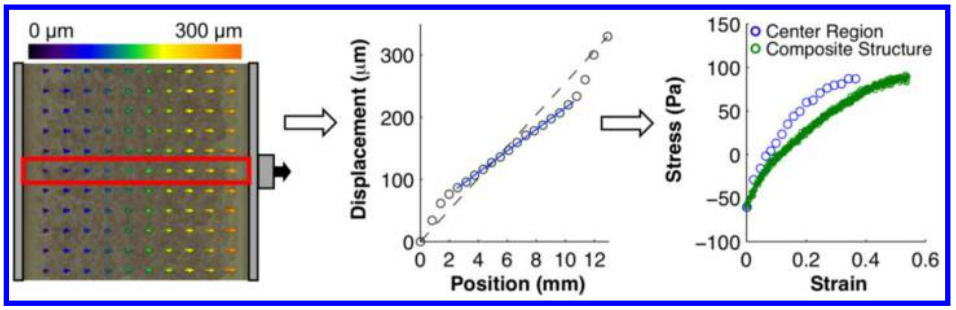

Figure 7. The deformation field obtained from PIV analysis between two successive images at low strain was superimposed on the pellicle (left). The magnitude of the displacement vectors in the red box were plotted as a function of position along the pellicle (center). The deformation was nonaffine (the dashed line represents affine deformation), and the regions near the two plates, at positions 0 and 13 mm, experienced a larger strain than the central region. Analysis of consecutive image pairs was used to calculate the mechanical properties of the center region of the pellicle (right) by using the local slopes from the displacement vs position plots. The different mechanical response of the center region compared with the entire pellicle indicates that the pellicle has a composite structure.

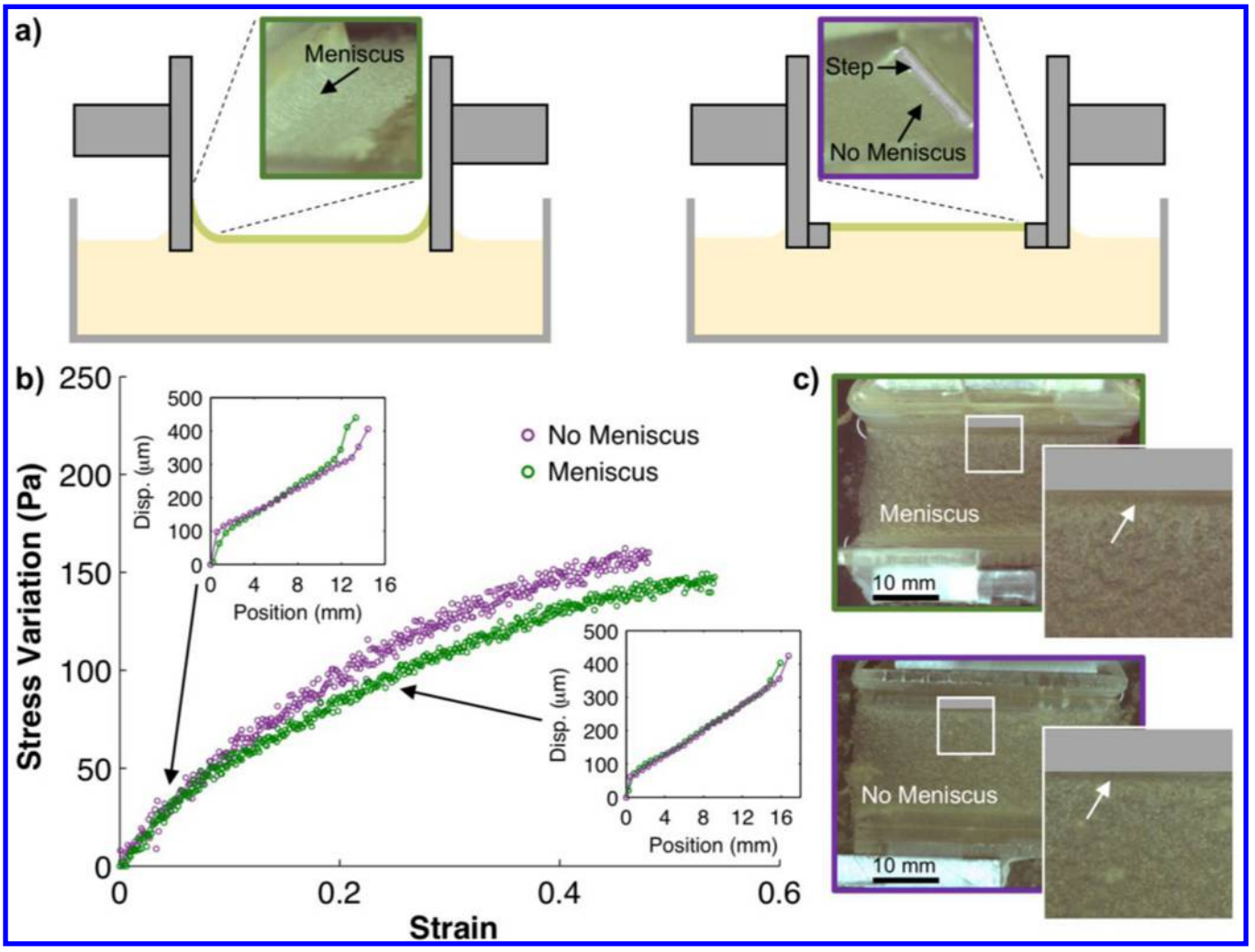

Figure 8. Two experimental setups to examine the effect of a meniscus (a) were used to obtain the stress−strain and displacement profile data in (b). The strain curves are represented as the change in stress from the initial growth-induced compressive stress. Top-down views highlighting the region of the pellicle near the attachment surface in each apparatus are shown in (c). In these images, the pellicles are at a strain of approximately 0.4, close to the point of detachment.

For example, there could be a different innate arrangement of bacteria and the extracellular matrix near the attachment surface, or the pellicle could be thinner or have a different surface roughness in this region, which was not taken into account in our stress calculation. Because the PIV analysis gave us the local strain within the pellicle, we used these data to calculate the apparent mechanical properties of different regions within the pellicle. For example, the right panel in Figure 7 shows the stress−strain curve for the center region of the pellicle, which has a locally linear deformation profile. Compared with the stress−strain curve for the composite pellicle structure, which was calculated using the average strain

DOI: 10.1021/acs.jpcb.6b02074
J. Phys. Chem. B XXXX, XXX, XXX−XXX

for the entire pellicle, the slope of the curve for the center region is steeper. This corroborates that compared with the effective properties that are measured for the whole pellicle, the center region of the pellicle is stiffer. Conversely, the portion of the pellicle near the attachment surface must be softer. Overall, our results show that the pellicle has a striated structure with mechanical properties that vary with distance from attachment surfaces.

Examining the displacement profiles further, we noticed that the center linear portion of the profile was flanked by two nonlinear regions that extended from the plates approximately 2 mm into the bulk of the pellicle. This length scale is roughly the meniscus size, as the capillary length of the medium is 2.3 mm.[19] Therefore, we hypothesized that this effect could be due to the formation of a different pellicle structure in the presence of a meniscus compared with the pellicle structure over a flat interface. Indeed, we previously observed that for highly wrinkled *B. subtilis* pellicles, the wrinkle pattern covering the meniscus region is different than the bulk of the pellicle, indicating a different formation process and pellicle structure than in the bulk.[19]

To test our hypothesis, we constructed a modified version of the experimental setup that eliminated the meniscus during pellicle growth (Figure 8a). While the original setup allowed the medium to naturally wet the plates and evaporate over time, the new setup had plates with a sharp corner to pin the medium contact line and create a flat interface. Additionally, we continuously injected medium to counteract evaporation and keep the interface flat during pellicle formation. The stress−strain curves for pellicles grown in the two different setups are shown in Figure 8b. It should be noted that the initial growth-induced compressive stress was different for the two experiments (approximately −60 Pa with the meniscus and −90 Pa without the meniscus). Therefore, the stress−strain curves are shown as the change in stress from the initial compressive state. This highlights the similarity between the two responses, which indicates that the composite mechanical response of the pellicle is independent of the presence of a meniscus. The insets show the displacement profiles during elongation at lower strains of 0.05−0.08 (left inset) and higher strains of 0.25−0.28 (right inset) for the two cases. When the pellicle grew with a meniscus, at low strains the nonlinear portion of the displacement profile extended approximately 2 mm into the bulk, and at higher strains this extension was reduced. This may be due to the curved surface of the pellicle on the meniscus becoming more flat as the pellicle is initially stretched, with this effect becoming diminished at higher strains once the pellicle is more elongated. With no meniscus at the attachment surface, however, we clearly observed that the deformation was still nonaffine and that the extension of the nonlinear portion did not depend on the strain. Overall, the composite mechanical response and displacement profiles were highly similar whether the pellicle grew in an environment with or without a meniscus, implying that this is not a key factor in the formation of a mechanically heterogeneous pellicle.

Furthermore, during experiments both with and without a meniscus, as we stretched the pellicle until it was near detachment, we observed a darker, smoother region right next to the plate that was morphologically different than the bulk of the pellicle (Figure 8c). This indicates that the pellicle structure near attachment surfaces is different than the rest of the pellicle and that the formation of this region is independent of the interface shape at the attachment surface. We hypothesize that the structure we observed in this region is what gives the pellicle more pliability at the edges, as seen in the deformation profiles. It remains to be determined whether this different structure is formed as a result of mechanical effects, genetic regulation, or other factors. For example, the compressive stress during pellicle growth may have a different effect on structure formation for portions of the pellicle attached to a solid surface compared with other portions surrounded by only pellicle. Alternatively, attachment to a surface may trigger the expression of different extracellular components, which is precedented in other species[37−39] and could result in a different chemical composition for this portion of the pellicle. Our results emphasize that we must take into account a heterogeneous mechanical response when studying biofilm detachment and inspire future work to determine the molecular basis of the structurally different layer of pellicle near the attachment surface.

■ CONCLUSIONS

In this study, we used a custom-built apparatus to probe the mechanical properties of *B. subtilis* pellicles. While most previous studies have focused on the viscoelastic properties of biofilms subjected to small deformations, we probed the mechanics at large deformations and made novel observations of visco-elastoplastic behavior with consequences for biofilm dispersal and removal. Most notably, pellicles exhibited plastic structural changes, meaning that if a biofilm is subjected to repeated deformations prior to detachment, it will have a different mechanical response with each deformation. This observation emphasizes the need to grow biofilms in situ prior to mechanical testing as opposed to transferring an already formed biofilm to an experimental apparatus, particularly since we observed that the greatest structural change occurs during the first loading cycle. Additionally, pellicles had striated mechanical properties and were more pliable near the attachment surface, indicating that when a mechanical force is applied to induce detachment, the biofilm will not deform uniformly. Overall, our results add to the growing fundamental understanding of biofilm mechanics, inform strategies to control biofilm dispersal, and inspire new approaches in both clinical and industrial settings for biofilm removal.

■ AUTHOR INFORMATION

Corresponding Author

*E-mail: eric.raspaud@u-psud.fr.

Notes

The authors declare no competing financial interest.

■ ACKNOWLEDGMENTS

E.C.H. gratefully thanks the Laboratoire de Physique des Solides at the Université Paris-Sud for hosting her during this collaborative study. We also thank Marion Lherbette for her contribution to the preliminary experiments. E.C.H. was supported by a fellowship from the Center for Molecular Analysis and Design at Stanford University. This work was supported by the Triangle de la Physique (2013-1028T) and by CNRS funding (Défi Instrumentation aux limites 2015-BIOFFORCE).

■ REFERENCES

(1) Stewart, P. S. Biophysics of Biofilm Infection. *Pathog. Dis.* **2014**, *70*, 212−218.

DOI: 10.1021/acs.jpcb.6b02074
J. Phys. Chem. B XXXX, XXX, XXX−XXX

(2) Kaplan, J. B. Biofilm Dispersal: Mechanisms, Clinical Implications, and Potential Therapeutic Uses. *J. Dent. Res.* **2010**, *89*, 205−218.
(3) Parsek, M. R.; Singh, P. K. Bacterial Biofilms: An Emerging Link to Disease Pathogenesis. *Annu. Rev. Microbiol.* **2003**, *57*, 677−701.
(4) Donlan, R. M.; Costerton, J. W. Biofilms: Survival Mechanisms of Clinically Relevant Microorganisms. *Clin. Microbiol. Rev.* **2002**, *15*, 167−193.
(5) Donlan, R. M. Biofilms and Device-Associated Infections. *Emerging Infect. Dis.* **2001**, *7*, 277−281.
(6) Kumar, C. G.; Anand, S. K. Significance of Microbial Biofilms in Food Industry: A Review. *Int. J. Food Microbiol.* **1998**, *42*, 9−27.
(7) Flemming, H.-C. Biofouling in Water Systems−Cases, Causes and Countermeasures. *Appl. Microbiol. Biotechnol.* **2002**, *59*, 629−640.
(8) Stewart, P. S.; Costerton, J. W. Antibiotic Resistance of Bacteria in Biofilms. *Lancet* **2001**, *358*, 135−138.
(9) Kaplan, J. B.; Ragunath, C.; Velliyagounder, K.; Fine, D. H.; Ramasubbu, N. Enzymatic Detachment of *Staphylococcus epidermidis* Biofilms. *Antimicrob. Agents Chemother.* **2004**, *48*, 2633−2636.
(10) Boyd, A.; Chakrabarty, A. M. Role of Alginate Lyase in Cell Detachment of *Pseudomonas aeruginosa*. *Appl. Environ. Microbiol.* **1994**, *60*, 2355−2359.
(11) Romero, D.; Aguilar, C.; Losick, R.; Kolter, R. Amyloid Fibers Provide Structural Integrity to *Bacillus subtilis* Biofilms. *Proc. Natl. Acad. Sci. U. S. A.* **2010**, *107*, 2230−2234.
(12) Roux, D.; Cywes-Bentley, C.; Zhang, Y.-F.; Pons, S.; Konkol, M.; Kearns, D. B.; Little, D. J.; Howell, P. L.; Skurnik, D.; Pier, G. B. Identification of Poly-N-Acetylglucosamine as a Major Polysaccharide Component of the *Bacillus subtilis* Biofilm Matrix. *J. Biol. Chem.* **2015**, *290*, 19261−19272.
(13) Hobley, L.; Ostrowski, A.; Rao, F. V.; Bromley, K. M.; Porter, M.; Prescott, A. R.; MacPhee, C. E.; van Aalten, D. M. F.; Stanley-Wall, N. R. BslA Is a Self-Assembling Bacterial Hydrophobin That Coats the *Bacillus subtilis* Biofilm. *Proc. Natl. Acad. Sci. U. S. A.* **2013**, *110*, 13600−13605.
(14) Branda, S. S.; Chu, F.; Kearns, D. B.; Losick, R.; Kolter, R. A Major Protein Component of the *Bacillus subtilis* Biofilm Matrix. *Mol. Microbiol.* **2006**, *59*, 1229−1238.
(15) Wilking, J. N.; Angelini, T. E.; Seminara, A.; Brenner, M. P.; Weitz, D. A. Biofilms as Complex Fluids. *MRS Bull.* **2011**, *36*, 385−391.
(16) Klapper, I.; Rupp, C. J.; Cargo, R.; Purvedorj, B.; Stoodley, P. Viscoelastic Fluid Description of Bacterial Biofilm Material Properties. *Biotechnol. Bioeng.* **2002**, *80*, 289−296.
(17) Wu, C.; Lim, J. Y.; Fuller, G. G.; Cegelski, L. Quantitative Analysis of Amyloid-Integrated Biofilms Formed by Uropathogenic *Escherichia coli* at the Air-Liquid Interface. *Biophys. J.* **2012**, *103*, 464−471.
(18) Hollenbeck, E. C.; Fong, J. C. N.; Lim, J. Y.; Yildiz, F. H.; Fuller, G. G.; Cegelski, L. Molecular Determinants of Mechanical Properties of *V. cholerae* Biofilms at the Air-Liquid Interface. *Biophys. J.* **2014**, *107*, 2245−2252.
(19) Trejo, M.; Douarche, C.; Bailleux, V.; Poulard, C.; Mariot, S.; Regeard, C.; Raspaud, E. Elasticity and Wrinkled Morphology of *Bacillus subtilis* Pellicles. *Proc. Natl. Acad. Sci. U. S. A.* **2013**, *110*, 2011−2016.
(20) Douarche, C.; Allain, J.-M.; Raspaud, E. *Bacillus subtilis* Bacteria Generate an Internal Mechanical Force Within a Biofilm. *Biophys. J.* **2015**, *109*, 2195−2202.
(21) Evilevitch, A.; Lavelle, L.; Knobler, C. M.; Raspaud, E.; Gelbart, W. M. Osmotic Pressure Inhibition of DNA Ejection From Phage. *Proc. Natl. Acad. Sci. U. S. A.* **2003**, *100*, 9292−9295.
(22) Leforestier, A.; Brasilès, S.; de Frutos, M.; Raspaud, E.; Letellier, L.; Tavares, P.; Livolant, F. Bacteriophage T5 DNA Ejection Under Pressure. *J. Mol. Biol.* **2008**, *384*, 730−739.
(23) São-José, C.; de Frutos, M.; Raspaud, E.; Santos, M. A.; Tavares, P. Pressure Built by DNA Packing Inside Virions: Enough to Drive DNA Ejection *In Vitro*, Largely Insufficient for Delivery Into the Bacterial Cytoplasm. *J. Mol. Biol.* **2007**, *374*, 346−355.
(24) Mullins, L. Softening of Rubber by Deformation. *Rubber Chem. Technol.* **1969**, *42*, 339−362.
(25) Dorfmann, A.; Trimmer, B. A.; Woods, W. A. A Constitutive Model for Muscle Properties in a Soft-Bodied Arthropod. *J. R. Soc., Interface* **2007**, *4*, 257−269.
(26) Dorfmann, A. L.; Woods, W. A.; Trimmer, B. A. Muscle Performance in a Soft-Bodied Terrestrial Crawler: Constitutive Modelling of Strain-Rate Dependency. *J. R. Soc., Interface* **2008**, *5*, 349−362.
(27) Muñoz, M. J.; Bea, J. A.; Rodríguez, J. F.; Ochoa, I.; Grasa, J.; Pérez del Palomar, A.; Zaragoza, P.; Osta, R.; Doblaré, M. An Experimental Study of the Mouse Skin Behaviour: Damage and Inelastic Aspects. *J. Biomech.* **2008**, *41*, 93−99.
(28) Gregersen, H.; Emery, J. L.; McCulloch, A. D. History-Dependent Mechanical Behavior of Guinea-Pig Small Intestine. *Ann. Biomed. Eng.* **1998**, *26*, 850−858.
(29) Horny, L.; Gultova, E.; Chlup, H.; Sedlacek, R.; Kronek, J.; Vesely, J.; Zitny, R. Mullins Effect in Aorta and Limiting Extensibility Evolution. *Bull. Appl. Mech.* **2010**, *6*, 1−5.
(30) Diani, J.; Fayolle, B.; Gilormini, P. A Review on the Mullins Effect. *Eur. Polym. J.* **2009**, *45*, 601−612.
(31) Lakes, R. *Viscoelastic Materials*; Cambridge University Press: Cambridge, U.K., 2009.
(32) Safari, A.; Tukovic, Z.; Walter, M.; Casey, E.; Ivankovic, A. Mechanical Properties of a Mature Biofilm From a Wastewater System: From Microscale to Macroscale Level. *Biofouling* **2015**, *31*, 651−664.
(33) Aggarwal, S.; Hozalski, R. M. Effect of Strain Rate on the Mechanical Properties of *Staphylococcus epidermidis* Biofilms. *Langmuir* **2012**, *28*, 2812−2816.
(34) Fung, Y. C. *Biomechanics*, 2nd ed.; Springer Science & Business Media: New York, 1993.
(35) Peterson, B. W.; Van der Mei, H. C.; Sjollema, J.; Busscher, H. J.; Sharma, P. K. A Distinguishable Role of eDNA in the Viscoelastic Relaxation of Biofilms. *mBio* **2013**, *4*, e00497-13.
(36) He, Y.; Peterson, B. W.; Jongsma, M. A.; Ren, Y.; Sharma, P. K.; Busscher, H. J.; van der Mei, H. C. Stress Relaxation Analysis Facilitates a Quantitative Approach Towards Antimicrobial Penetration into Biofilms. *PLoS One* **2013**, *8*, e63750−10.
(37) Belas, R.; Simon, M.; Silverman, M. Regulation of Lateral Flagella Gene Transcription in *Vibrio parahaemolyticus*. *J. Bacteriol.* **1986**, *167*, 210−218.
(38) Vandevivere, P.; Kirchman, D. L. Attachment Stimulates Exopolysaccharide Synthesis by a Bacterium. *Appl. Environ. Microbiol.* **1993**, *59*, 3280−3286.
(39) Otto, K.; Norbeck, J.; Larsson, T.; Karlsson, K. A.; Hermansson, M. Adhesion of Type 1-Fimbriated *Escherichia coli* to Abiotic Surfaces Leads to Altered Composition of Outer Membrane Proteins. *J. Bacteriol.* **2001**, *183*, 2445−2453.

DOI: 10.1021/acs.jpcb.6b02074
J. Phys. Chem. B XXXX, XXX, XXX−XXX